RSC Advances

ROYAL SOCIETY OF CHEMISTRY

www.rsc.org/advances

Synthesis and Properties of a Novel Ecofriendly Superabsorbent Hydrogel Nanocomposite Based on Xyloglucan-*graft*-poly(Acrylic Acid)/Diatomite

Jean Felix Mukerabigwi[†a], Shaojun Lei[†a], Haili Wang[†], Shiying Luo[†], Xiaoya Ma[†], Jing Qin[†], Xueying Huang[†], Yu Cao[†]*

†: Key Laboratory of Pesticide and Chemical Biology (Ministry of Education), College of Chemistry, Central China Normal University, Wuhan 430079, P. R. China

a: Equal contributors to the work.

*: To whom correspondence to be addressed.

E-mail: caoyu@mail.ccnu.edu.cn

Tel: +86-27-67867953

Abstract

Recently, there has been growing interest in the use of natural available materials to prepare superabsorbent, due to their low-cost and environmental friendliness. In this study, biodegradable organic-inorganic superabsorbent was prepared through graft copolymerization of acrylic acid (AA) onto xyloglucan (XG) polysaccharide chains, in the presence of diatomite as inorganic material, *N,N'*-Methylene-Bis-Acrylamide (MBA) as a cross-linker and ammonium persulphate (APS) as an initiator, in an aqueous solution (XG-*g*-PAA/Diatomite). The synthesized hydrogel nanocomposite was characterized with FTIR, SEM, TGA and XRD. In this contribution, the properties such as swelling and water retention behavior of the XG-*g*-PAA/Diatomite were investigated. Moreover, the influence of each starting material content on water absorbency property of XG-*g*-PAA/Diatomite composite was systematically studied. The results showed that the composite water absorbency capacity was 1057.06 ± 69.53 g/g in deionized water and 65.67 ± 5.43 g/g in 0.9 wt.% NaCl saline solution under the optimized conditions. The excellent properties of the prepared SAP composite suggested that it could find diverse range of applications such as in hygienic products, agriculture and waste-water treatment. Furthermore, being biodegradable and low-cost could be the added advantages for XG-*g*-PAA/Diatomite superabsorbent composite.

Keywords: Xyloglucan, diatomite, acrylic acid, superabsorbent, biodegradable.

1 Introduction

Superabsorbent polymers (SAPs) are soft materials that have the ability to absorb and retain large volumes of water and aqueous solutions from tens to thousands times of their own weight in a relatively short time, and retain a swollen state even under some pressure.[1] This makes them ideal for use in water absorbing applications such as baby nappies and adults incontinence pads to absorbent medical dressings, controlled release medium, agriculture and horticulture, and pharmaceutical applications, etc.[2,3] However, most of the SAPs are based on fully petroleum-based polymers, which are reported to be costly, poorly degradable, and environmental unfriendly.[4,5] Moreover, given the gradual depletion of petroleum resources and the growing environmental pollution crisis from polymer syntheses, the utilization of low-cost and biodegradable resources for preparing SAPs, based on natural materials has become the focus of current studies.[6,7]

In this regard, the use of polysaccharides and substitutes for petroleum-based polymers has academically as well as industrially drawn a considerable attention. Moreover, these compounds have greater commercial and environmental values, along with the advantages of having low production costs, non-toxicity, higher renewability, and better biodegradability when SAPs are derived from polysaccharides.[8] In spite of these polysaccharide based SAP advantages, the lower swelling behavior and gel strength of these SAPs severely restrict their application.[9] Therefore, numerous approaches have been recently studied for the development of economic and more effective polysaccharide based SAP hydrogels. Particularly, the introduction of inorganic fillers to a polymer matrix has been considered as a possible candidate for fabricating polysaccharide based SAP hydrogel with improved strength and stiffness. Among inorganic compounds, special attention has been paid to clay minerals which are easily available on market for use in nanocomposites, due to their small particle size and intercalation properties.[10] Therefore, the incorporation of both

biopolymer and inorganic nanoparticles into SAP synthetic components through slight modifications of their structures is a cost effective approach to enhance properties of the existing superabsorbents.

Typically, since SAP are hydrophilic polymer network lightly cross-linked in some fashion to produce an elastic structure.[11] In preparation point of view, these materials could be produced by carrying out free radical cross-linking polymerization. According to the literature, Pourjavadi and Mahdavinia[8] reported that graft copolymerization of vinyl monomers onto polysaccharides is an efficient route for the preparation of hybrid hydrogels *i.e.* hydrogel composed with both synthetic polymers and biopolymers. This could be achieved by covalent coupling of several reactive functional groups of vinyl monomers within the backbone chain groups of biopolymer in the presence of a free radical initiator.[12,13]

Diatomaceous earth ($SiO_2.nH_2O$) also known as diatomite is a naturally occurring siliceous sedimentary rock that is easily crumbled into a fine white powder. The typical chemical composition of the diatomaceous earth is comprised of 86% silicon, 5% sodium, 3% magnesium and 2% iron.[14,15] The silica surface of diatomite is covered by reactive silanol (Si-OH) groups. Its highly porous structure, low density and high surface area results in a number of industrial applications, such as filtration media for various inorganic and organic chemicals and as absorbents, catalyst carriers, fillers and so on.[16] Therefore, due to its hydrophilic property, large availability in many areas of the world, chemical stability, extremely low cost and non-toxicity, this fossil material is an ideal component for added superabsorbent network to improve the swelling properties. Moreover, the porous structure of diatomite allows a large amount of water to penetrate into the polymer network and may be of benefit to water absorbency of corresponding superabsorbent.[17]

Xyloglucan is a neutral, non-toxic water soluble polysaccharide, whose degradation products consist of naturally occurring saccharides.[18] Xyloglucan, is the major storage polysaccharide present in the seeds of the tamarind tree (*Tamarindus indica*), and tamarind kernel powder is the xyloglucan rich raw-material commercially available.[19] It is composed with a polysaccharide which has 1,4-β-D-glucan backbone partly substituted by 1,6-α-D-xylopyranosyl side-chains, some of which are further substituted by 1,2-β-D-galactopyranosyl residue.[20] The present available applications of xyloglucan we can list: controlled release drug,[21] common additives for food, cosmetics and textile,[22] tissue engineering,[23] waste-water treatment,[24] and so on. However, the comprehensive literature survey reveals that there is no published report regarding the use of xyloglucan into organic-inorganic SAP nano-composite.

The present work aims to develop the synthesis of a novel organic-inorganic superabsorbent composite by graft copolymerization reaction of partially neutralized acrylic acid (AA) and xyloglucan (XG) polysaccharide, using *N,N′*-Methylene-Bis-Acrylamide (MBA) as a cross-linker and ammonium persulphate (APS) as an initiator in the presence of diatomite as inorganic nano-filler (XG-*g*-PAA/Diatomite), in aqueous solution. Through this study, properties such as swelling and water retention behavior of the prepared SAP were investigated. Furthermore, the relationship between the amount of each starting material (such as initiator, cross-linker, polysaccharide, diatomite) and the water absorbency of the synthesized SAP composite was studied in both deionized water and 0.9 wt.% NaCl saline solution. In addition, the effect of clay content to the water retention capacity of the composite was investigated and discussed.

2 Materials and methods

2.1 Materials

Raw diatomite purchased from Linjiang City Tianyuan Catalyst Co., Ltd (China) was purified before use, through calcination and hot acid leaching. Xyloglucan (Food grade) was obtained from Henan Anrui Biotechnology Co., Ltd (China). Acrylic Acid (CP grade), Ammonium Persulfate (AR grade), *N,N'*-Methylene-Bis-Acrylamide (CP grade) and Hydrochloric Acid (AR grade) were all supplied by Sinopharm Reagent Co., Ltd (China). Sodium Hydroxide (AR grade) was obtained from Tianjin Fu Chen Chemical Reagent Factory (China). All other chemicals were commercially available analytical grade reagents unless otherwise stated.

2.2 Methodology

2.2.1 Diatomite purification

The raw diatomite powder was treated in hot-acid leaching solution and then through calcination to remove impurities such as alumina, alkaline earth and alkali metal compounds. The raw diatomite was screened through a sieve of 45 µm aperture and leached in 5 M HCl solution under oil bath at 100°C for 1 h. During leaching, 60 g of diatomite sample was weighed and poured into 300 ml of solution, then the solution was stirred continuously at 500 rpm using a magnetic stirrer and a thermostat was used to keep the reaction medium at constant temperature. After a predetermined period of time, the solid product was filtered and washed 4 times with 200 mL deionized water each time. Then the filtrate was calcined in a muffle furnace (G WL-80, Hengtai HSBC Branch, China). The instrument was programmed such that it provided heating from 25°C to 500°C by 20°C/min rate and remains at 500°C for 2 h. Thereafter, the product was cooled down at room temperature and at the same rate, grinded and then screened through the 45 µm sieve.

2.2.2 Preparation of XG-*g*-PAA/Diatomite SAP composite

The superabsorbent (XG-g-PAA/Diatomite) was obtained through graft copolymerization of AA onto XG polysaccharide chains, in the presence of APS as initiator, MBA as cross-linker and diatomite as inorganic nanoparticles. Schematically, the general preparation procedure for XG-g-PAA/Diatomite was shown in Scheme 1. Typically, a series of samples with various amounts of XG (8-14 wt.%), diatomite (9-18 wt.%), cross-linker (MBA: 0.03-0.06 wt.%), initiator (APS: 0.5-0.8 wt.%), and AA monomers (15 g) (the wt.% referred hereinafter was based on 15 g of AA monomer content in the reaction system) with various degree of neutralization (70-85%) were prepared by the following procedure: Desired amount of XG was weighed and dispersed into 100 mL deionized water and the aqueous solution was put in a 250 mL four-necked flask equipped with a stirrer, a condenser, a thermometer, and a nitrogen line. The slurry was heated to 90°C for 30 min under nitrogen atmosphere and oil bath to completely dissolve XG into water. Thereafter, the temperature was cooled down to 65°C, then the cross-linker (MBA) dissolved into 15 g of the partially neutralized AA (AA was neutralized with 25% of NaOH under ice water bath with magnetic stirring), under ultrasonic machine and mechanical stirring for 10 min, was poured into the solution and then the diatomite was added to the mixture solution. After 15 min, the initiator APS (dissolved into 5 mL deionized water) was added to the mixture to generate radicals and allowed to react for 5 h at 65°C to ensure the completion of the graft copolymerization. Then the resulting product was cut into two halves which were cast into petri dishes (diameter ~20 cm) and then dried in an oven at 85°C to a constant weight for 24 h to evaporate the solvent. The dried product was milled and screened. All samples used had a particle size in the range of 40–80 mesh.

2.2.3 Characterizations

The structure of the samples was recorded on an FTIR spectrometer, Spectrum-2000, (PerkinElmer, Japan). The samples were powdered and mixed with KBr (spectroscopic grade) and

then pressed into a 1 mm pellets. The spectra of the samples were recorded at 4 cm^{-1} resolution; 32 scans were averaged to reduce the noise. Spectra were then truncated to cover only the 4000 to 500 cm^{-1} range.

The composite surface morphological studies were determined by using Scanning electron microscope, Quanta 450 FE G, (FEI Hong Kong Limited, China). Prior to scanning, the samples were sputter-coated with a thin layer of gold and the morphology of the composite was observed at 5 kV accelerating voltage and high magnification of 5,000 X.

The Thermo Gravimetric Analysis (TGA) of the composites was carried out using the NETZSCH STA 409 PC (Germany) analyzer in an atmosphere of nitrogen. The samples were subjected to heating in a range of 30º - 600ºC at a rate of 10ºC/min.

The X-Ray Diffraction (XRD) studies of the composites have been performed using the Rigaku, MiniFlex 600, Japan equipped with Cu Kα radiation source, operated at 40 Kv and 15 mA. The diffraction data were acquired in the range of $2\theta = 0.02^{o}$, 4 s steps and in the angular region between 2–50^{o}.

2.2.4 Water absorbency measurement

The water absorbency test of the prepared SAP was determined in deionized water as well as in saline solution of 0.9% NaCl as follow: Accurately weighed 0.1±0.001 g samples were immersed into beakers containing 400 ml of deionized water or in 250 mL of 0.9% NaCl solution and allowed to swell at room temperature for 24 h to reach the swelling equilibrium. The swollen hydrogels were filtered through a 100-mesh screen to remove the non-absorbed water and weighed. The water absorbency was calculated by the following equation:

$$Q_{eq} = \frac{M_1 - M_0}{M_0} \quad (1)$$

Where Q_{eq} is the water absorbency, M_1 is the weight of the swollen hydrogel, and M_0 is the weight of dry sample. Q_{eq} was calculated as grams of water per gram of sample.

2.2.4 Water retention measurement

The water retention behavior of the prepared SAP was determined at two different fixed temperatures *i.e.* 45°C and 60°C. Accurately weighed 50 g fully swollen hydrogels were put into beakers and placed into an oven at a fixed temperature. The water retention study was measured as a function of time by gravimetry. The percentage water retention (W_R) of the superabsorbent was calculated every 1 h, according to equation (2):

$$W_R(\%) = \frac{W_i}{W_0} \times 100 \quad (2)$$

Where W_0 is the initial weight of the fully swollen superabsorbent samples in deionized water and W_i is its weight after loss of water at each time interval.

3 Results and Discussion

3.1 Mechanism of XG-*g*-PAA/Diatomite SAP formation

Schematically, the proposed mechanism of graft polymerization of AA onto the polymeric chains of XG in the presence of diatomite as inorganic nano-filler by using of APS as a free radical initiator and MBA as a hydrophilic cross-linker was illustrated in scheme 1. Briefly, sulfate anion radical generated from the hemolytic cleavage of APS initiator, reacts and gives rise to hydroxyl free radical.[25] The sulfate anion radical abstracts hydrogen from the hydroxyl group of the XG to form alkoxy radicals on the substrate. Therefore, this persulfate-saccharide redox system results in

192 active centers on the substrate to radically initiate polymerization of a partial pre-neutralized AA
193 with NaOH leads to a graft copolymer of PAA onto XG backbone chains.[26] During chain
194 propagation cross-linker end groups may react with the polymer chain. The copolymer formed in
195 this way consisted of a cross-linked structure as the MBA was present in the system. Since the
196 diatomite used as inorganic filler present highly active –OH group, which could participate in the
197 reaction system through chemical bonding with carboxylate group of grafted PAA. Thus, the
198 diatomite particles may act as crosslinking point in the network and through this process, XG-*g*-
199 PAA/Diatomite SAP was formed.

200

201 **Scheme I.** Proposed mechanism pathway for the synthesis of biodegradable organic-inorganic SAP
202 (XG-*g*-PAA/Diatomite) superabsorbent composite through graft copolymerization

203 **3.2 FTIR analysis**

204 The FTIR spectra of diatomite, XG, XG-*g*-PAA and XG-*g*-PAA/Diatomite are shown in Fig.1.
205 In the FTIR spectrum of diatomite (Fig. 1a), the absorption band at ~3439 cm $^{-1}$ and ~1635 cm^{-1} are
206 ascribed to the –OH stretching and bending vibration of adsorbed water on the silicate surface. The
207 bands at ~1104 cm^{-1} and 800 cm $^{-1}$ reflect the asymmetric and symmetric stretching modes of
208 siloxane group (-Si-O-Si-) bonds, respectively.[27,28] Fig. 1b displays the FTIR spectrum of XG, the
209 absorption bands at ~3421 cm $^{-1}$ was assigned to the stretching vibration of –OH group, ~2926 cm^{-1}
210 was ascribed to the absorption peak of –CH, ~1646 cm^{-1} could be attributed to the bending
211 vibrations of –OH groups. Fig. 1c shows the FTIR spectrum of prepared SAP without diatomite
212 (XG-g-PAA), the bands at 3425 cm^{-1}was assigned to –OH, 2941 cm^{-1} could be attributed to the
213 stretching vibration of –CH bonds. Compared to XG spectra in Fig. 1b, it can be seen that the

absorption band of XG at 1015 cm^{-1} (stretching vibration of C–OH groups) disappeared after reaction, and the bands at 1119 and 1061 cm^{-1} and (asymmetrical stretching vibration of C–O–C) appeared in Fig. 1c about the spectra of XG-*g*-PAA, indicating that XG has reacted with PAA with its reactive –OH groups. Moreover, the two new bands around 1571 cm^{-1} and 1415 cm^{-1} appeared in Fig. 1c are due to the asymmetrical and symmetrical stretching modes of the $–COO^-$ groups, this information indicates that PAA had been grafted onto XG backbone.[29] Fig. 1d represents the spectrum of XG-*g*-PAA/Diatomite, compared to the spectrum in Fig. 1c two new peaks 1056 cm^{-1} and 790 cm^{-1} appeared, which could be attributed to the asymmetric and symmetric stretching modes of siloxane group (-Si-O-Si-) bonds found in diatomite, respectively. Additionally, a new absorption peak appeared at 1673 cm^{-1} may be attributed to the reaction between carboxylate group of PAA and hydroxyl group on diatomite. Therefore, the above FTIR characterization suggested that the desired product was successfully synthesized.

Fig.1: The FTIR spectra of (a) Diatomite, (b)XG, (c) XG-*g*-PAA, (d) XG-*g*-PAA/Diatomite (12 wt.%).

3.3 TGA analysis

The thermal decomposition behavior of XG, and the SAP composite prepared with 0, 12, and 18 wt.% diatomite were studied by the TG analysis and the results were shown in Fig. 2. The initial decomposition of both the samples is due to the presence of little bit of moisture in the samples. However, from Fig. 2 it is clearly shown that the thermal stability of the SAP composite prepared with clay content (diatomite) is higher that the SAP composite prepared without the diatomite.

Moreover, the thermal stability of the composite prepared at the optimized conditions *i.e,* with 12 wt.% diatomite showed higher thermal stability compared to the SAP composite prepared with higher diatomite content (18 wt.%). Thus, the higher thermal stability of the composite synthesized at optimized condition could be an added advantage as it may resist the high temperature through different applications.

Fig. 2: TGA curves of XG, XG-*g*-PAA, XG-g-PAA/Diatomite (12 wt.% diatomite), and XG-*g*-PAA/Diatomite (18 wt.% diatomite)

3.4 XRD analysis

The XRD diffraction patterns of XG, diatomite, XG-*g*-PAA and XG-*g*-PAA/Diatomite were determined and presented in Fig. 3a-d, respectively. From Fig. 3a and Fig. 3b, it is easy to find that the XRD curves of XG and diatomite show the strong characteristic peaks at 2 θ=20.06^{o} and 2 θ=23.7^{o}, respectively. From Fig. 3c and Fig. 3d, it is interesting to note that there is no obvious characteristic peak of XG and diatomite observed in the XRD diffraction patterns of SAP composites prepared with 0 wt.% and 12 wt.% of diatomite, respectively. It has been reported that the nanocomposite should be classified as exfoliated or intercalated based on the absence of 001 reflection.[30] Thus, the disappearance of characteristic peaks of XG and diatomite in the XRD diffraction patterns of XG-*g*-PAA and XG-*g*-PAA/diatomite clearly reveals the exfoliation and substantially dispersion of XG and diatomite in polymeric matrix of the synthesized SAP composites during the polymerization process.

Fig. 3: XRD diffraction patterns of (a) XG, (b) Diatomite, (c) XG-*g*-PAA, and (d) XG-*g*-PAA/Diatomite (12 wt.% Diatomite)

3.5 SEM observations

Scanning electron micrographs of diatomite and composite superabsorbents containing 0 wt.% (XG-*g*-PAA) and 12 wt.% diatomite (XG-*g*-PAA/diatomite) are depicted in Fig. 4a-c, respectively. It is evident from the Fig. 4a that the disc-shaped structure of diatom is clearly shown, and the diatomite SEM image exhibits diatomite frustules with closed pores dispersed in clay and some other fine particles.[28] Obviously, from Fig. 4b-c, the fracture surface morphology of the XG-*g*-PAA composite is different from that of XG-*g*-PAA/Diatomite. It can be observed that the XG-*g*-PAA composite (Fig. 4b) displays a smooth and tight fracture surface without any pores. However, the composite containing diatomite (Fig. 4c) presents a loose and porous fracture surface. This fracture surface is convenient for the penetration of water into the polymeric network, and may be of benefit to water absorbency of corresponding superabsorbent.[31] In Fig. 4c, the disc-shaped structures of diatom and its closed pores can also be seen dispersed into the composite polymeric matrix.

Fig. 4: Scanning Electron Micrographs of (a) Diatomite, (b) XG-*g*-PAA, and (c) XG-*g*-PAA/Diatomite (12 wt.%)

3.6 Effect of XG content on water absorbency

The effect of XG content on the water absorbency capacity of XG-*g*-PAA/Diatomite composite was studied in deionized water as well as in 0.9 wt.% NaCl saline solution, by preparing several SAP composites with various amount of XG content (*i.e.* 10, 12, 14, 16, and 18 wt.% of the

monomer), and keeping constant other factors such as initiator (0.7 wt.%), cross-linker (0.05 wt.%), neutralization degree (80%), diatomite (14 wt.%) and AA (15 g). The results for this test were depicted in Fig. 5, as it can be seen that the water absorbency of the XG-*g*-PAA/Diatomite SAP composite in both deionized water and saline solution was increasing with the raising of XG content up the equilibrium value of 14 wt.%, as the highest water absorbency was achieved when the XG-*g*-PAA/Diatomite SAP composite was prepared with 14 wt.%, then a significant decrease in water absorbency was remarked with further increment of XG content into the superabsorbent polymer matrix. This fact may be explained as follow:

It is interesting to note that XG structure contains a number of hydrophilic groups such as –OH group which could react with PAA $–COO^-$ groups to enhance the polymeric network resulting in an increased water absorbency capacity of XG-*g*-PAA/Diatomite SAP composite when the XG was raised from 10 to 14 wt.%.[31] Additionally, when the amount of XG was below the equilibrium value (*i.e.* <14 wt.%), the monomer in the reaction system was in excess. Hence, the overmuch AA turned to be a homopolymer, which cannot contribute to the water absorbency.[32] On the other hand, when the content of XG was >14 wt.% in the SAP composite feed, the decrease of water absorbency in both deionized water and 0.9 wt.% NaCl saline solution could be attributed to the generation of more crosslink points in the polymeric network, inducing an increase in crosslink density of the composite, therefore, a decrease in the elasticity of the polymer.[31,33] Moreover, under higher XG concentration in the reaction system may partly physically intercalate in the composite polymeric network, thus a decrease of water absorbency capacity tendency of the XG-*g*-PAA/Diatomite SAP composite was remarked at the XG content beyond the optimum value of 14 wt.%.

Fig. 5: Effect of XG content on the water absorbency. (Data were given as means ± SD (n = 3)). AA=15 g, diatomite=12 wt.%, MBA=0.05 wt.%, APS=0.7 wt.%, reaction temperature 65°C, neutralization degree=80%

3.7 Effect of initiator content on water absorbency

The graft copolymerization was chemically initiated by APS oxidizer to dissociate dianion in the composite and generate free radicals. The results about the effect of the initiator content on swelling behavior of XG-g-PAA/Diatomite SAP composite are represented in Fig. 6. The water absorbency capacity of the composite in both deionized water and 0.9 wt.% NaCl saline solution was increasing with the increase of the APS amount from 0.5 to 0.7 wt.%. The further increase of APS in the composite resulted into an obvious decrease of water absorbency of the composite. From Fig. 6, it can be seen that the water absorbency of XG-*g*-PAA/Diatomite SAP composite at equilibrium value (0.7 wt.% APS) was 1057.06 ± 69.53 g/g and 65.67±5.43 g/g in deionized water and 0.9 wt.% NaCl saline solution, respectively. Thereafter, the slight increase of initiator from 0.7 wt.% (0.105 g APS) to 0.8 wt.% (0.120 g APS) leads to a tremendous decrease in water absorbency from 1057.06 ± 69.53 g/g to 449.64±23.33g/g (*i.e.* the water absorbency was reduced by 57.46%) in deionized water. The similar observation was remarked in water absorbency of the composite in 0.9 wt.% NaCl saline solution as it was reduced by 25%.

The possible way to explain this, is that when the amount of APS was below the optimum value (<0.7 wt.%) in the feed, the number of free radicals was not enough to efficiently form the polymer network during free radical polymerization reaction, which resulted into a decreased water absorbency capacity of XG-*g*-PAA/Diatomite SAP composite.[34,35] Moreover, under the low concentration of initiator, the copolymerization reaction is slower and leads to the fewer polymer

network with low molecular weight, thereby decreasing the water absorbency of the obtained hydrogel. On the other hand, the higher concentration of APS in the reaction system (>0.7 wt.%), the growing macromolecular chains are terminated at a faster rate which may also lead to the formation of low molecular weight polymer with small polymer network space, thus, the decrease in the water absorbency of the composite was noticed.[34,36]

Fig. 6: Effect of initiator (APS) content on the water absorbency. (Data were given as means ± SD (n = 3)). AA=15 g, diatomite=12 wt.%, MBA=0.05 wt.%, XG=14 wt.%, reaction temperature 65°C, neutralization degree=80%

3.8 Effect of cross-linker content on water absorbency

It was reported that a relatively small amount of the cross-linker could have a great effect on the properties of the resulting SAP.[37] The effect of MBA content on water absorbency of XG-*g*-PAA/Diatomite SAP composite in deionized water and 0.9 wt.% NaCl saline solution was studied in the range of 0.03 to 0.07 wt.% and the results were shown in Fig. 7. From Fig. 7, it is easy to find that the water absorbency capacity of XG-*g*-PAA/Diatomite SAP composite was improving when the MBA content was increased from 0.03 to 0.05 wt.%. Thereafter, the MBA content beyond 0.05 wt.%, a gradual decrease in water absorbency in both deionized water and 0.9 wt.% NaCl saline solution was noticed. Typically, a cross-linker is used through SAP preparation to provide crosslinks between polymer chains to form a three-dimensional network and prevent the SAP swelling to infinity *i.e.* dissolving. According to Flory theory[38] about the relationship between the swelling ratio and network structure parameter for the swelling of ionic network, it was described that the absorption ratio of hydrogel is directly related to the relation of the ionic osmotic pressure

and cross-linked density, as well as the affinity of the hydrogel with water. In our study, when the MBA content was below the optimum value (<0.05 wt.%), the low water absorbance of the composite could be explained by the relatively low degree of cross-linking between polymer chains, which may contribute to the increased number of dissoluble materials into the XG-*g*-PAA/Diatomite SAP composite three-dimension network. In contrast, when the amount of MBA was high *i.e.* >0.05 wt.%, the high strength of the XG-*g*-PAA/Diatomite, defined by the high cross-linking density, contributed to a decreased space between polymer networks, which resulted into a decrease water absorbency of the composite. Therefore, it should be pointed out that the increase of cross-liking density (above the optimum value) results into formation of increased gel strength with decreased swelling ratio. The similar observation was found in the study conducted by.[39,40]

Fig. 7: Effect of Cross-linker (MBA) content on the water absorbency. (Data were given as means ± SD (n=3)). AA=15 g, diatomite=12 wt.%, APS=0.7 wt.%, XG=14 wt.%, reaction temperature=65°C, neutralization degree=80%

3.9 Effect of neutralization degree of AA on water absorbency

Fig. 8 displays the results of the effect of AA neutralization percentage (in the range of 70-90%) on the swelling ration of XG-*g*-PAA/Diatomite SAP composite in deionized water as well as in 0.9 wt.% NaCl saline solution. Obviously, it can be seen that the swelling ratio of the composite increased from 455 g/g to 1057 g/g and from 48 g/g to 67 g/g in deionized water and 0.9 wt.% NaCl saline solution, respectively, when the AA neutralization percentage was increased from 70% to the equilibrium value of 80%. Then, further increase of AA neutralization percentage resulted

into a gradual reduction of the swelling ratio of the composite in deionized water and in 0.9 wt.% NaCl saline solution. This can be interpreted in terms of electrostatic repulsion into the XG-g-PAA/Diatomite polymer composite. When the AA is neutralized by NaOH, the AA carboxylic acid group turns into carboxylate group. Then, the negatively charged carboxyl groups attached to the polymer chains set up an electrostatic repulsion, which tended to expand the network. In a certain range of neutralization degree, the electrostatic repulsion increased with the increase of neutralization degree, resulting in the increase of water absorbency. However, further increases in the neutralization degree of PAA *i.e.* beyond the optimum value, may result into the generation of more sodium ions, which lead to a reduced electrostatic repulsion by screening the negative charges of carboxyl groups, thus resulting in the decrease of water absorbency. [41]

Fig. 8: Effect of AA neutralization percentage on the water absorbency. (Data were given as means ± SD (n = 3)). AA=15 g, diatomite=12 wt.%, APS=0.7 wt.%, XG=14 wt.%, reaction temperature 65°C, MBA=0.05 wt.%.

3.10 Effect of diatomite content on water absorbency

The effect of diatomite content on swelling ration was investigated in deionized water and 0.9 wt.% NaCl saline solution, to the SAP prepared with various amount of diatomite in the composite feed *viz.* 0, 3, 6, 9, 12, 15, and 18 wt.%. As it can be seen from Fig. 9, the swelling ratio of the composite was increasing with the increase of diatomite content from 0 to 12 wt.%, and then further increase of diatomite caused an obvious decrease of the composite water absorbency capacity, in both water and 0.9 wt.% NaCl saline solution. This mechanism could be due to the way that the inorganic clay such as diatomite mineral particle in network acts as an additional network point.[34]

This could take place through the chemical bonding between the –OH group of diatomite with the –COO^- group of grafted PAA. Due to this fact, it is worthy to point out that the clay (diatomite) and cross-linker (MBA) content into the feed of the composite should have the same effect on swelling ratio of the hydrogel as both they may contribute the cross-linking density of the hydrogel polymer networks. Therefore, the use of diatomite into the preparation of XG-*g*-PAA/Diatomite, cannot only improve the swelling ratio of the composite due to its hydrophilic –OH groups but also, it can enhance the gel strength of the composite network as it may increase the cross-linking density. However, according to our results from Fig.9, it was revealed that an excessive increase of diatomite content in the feed (>12 wt.%) resulted into hydrogel with swelling ratio lower that the composite prepared without diatomite *i.e.* XC-*g*-PAA SAP composite.

Fig. 9: Effect of clay content (diatomite) on the water absorbency. (Data were given as means ± SD (n = 3)). AA=15 g, neutralization degree=80%, APS=0.7 wt.%, XG=14 wt.%, reaction temperature 65°C, MBA=0.05 wt.%.

3.11 Water retention test results

The water retention is one of the key properties of the hydrogel in the various applications. Generally, the water retention of organic-inorganic hybrid SAP was studied in several researches from the literature.[42] However, few reports are available about the exact effect of clay content on water retention of the obtained SAP. In this study, we assessed the influence of clay content on water retention of the XC-*g*-PAA/Diatomite SAP composite prepared with various amount of diatomite *i.e.* 0, 6, 9, 12, 15, and 18 wt.%. The water retention of each SAP sample prepared was

studied at two different fixed temperatures *viz.* 45°C and 60°C, and the results for this experiment were collected in Fig. 10a-f. As it can be seen from Fig. 10a-f, the SAP retained water was gradually decreasing as the time was increasing. Nearly all samples, the retained water was completely evaporated after 11 h and 8 h when the sample was incubated into the oven heated at 45°C and 60°C, respectively. Specifically, while comparing Fig. 10a and Fig. 10d *i.e.* the water retention curve of the SAP composite prepared with 0 wt.% (without diatomite) and 12 wt.% (diatomite optimum value), respectively, it is interesting to note that at 60°C and after 7 h, the SAP composite prepared without diatomite (Fig. 10a), 0.89% of the water was remaining, whereas, at the same predicted time and temperature all the absorbed water was completely evaporated for the SAP composite prepared with 12 wt.% diatomite. However, the difference of water retention of these two different types of SAP composite is slightly small; this phenomenon should be explained by the presence of loosely porous surface of the XC-*g*-PAA/Diatomite SAP composite which may provide enlarge space for the absorbed water evaporation at high temperature such as 60°C. These results are in good agreement with the SEM observation of the two composites (Fig. 4b-c).

Interestingly, at the lower temperature of 45°C, the SAP composite prepared with 12 wt.% (Fig. 10d) diatomite was revealed to perform better that the SAP composite synthesized without clay content (Fig. 10a), in times of water retention. After 10 h, the remaining water was found to be 0.60% and 0.27%, respectively. This fact should be attributed to the higher mechanical strength between polymeric networks of the SAP composite prepared with a certain amount of inorganic clay material as it may act as an additional network point as previously discussed and also contribute to the enhanced thermal stability behavior of such SAP composite. Generally, the composites exhibited excellent water retention capacity at both temperatures. However, based on

433 the results of this experiment, there was no obvious effect of clay content (diatomite) on the water
434 retention property of the XG-*g*-PAA/Diatomite SAP composite.

435

436 Fig. 10: Water-retention properties of XG-*g*-PAA/Diatomite SAP prepared with various amount of
437 diatomite at 45°C and 60°C. (a): 0 wt.% diatomite; (b): 6 wt.% diatomite; (c): 9 wt.% diatomite; (d):
438 12 wt.% diatomite; (e): 15 wt.% diatomite; (f): 18 wt.% diatomite. (Data were given as means ± SD
439 (n = 3)). AA=15 g, neutralization degree=80%, APS=0.7 wt.%, XG=14 wt.%, reaction temperature
440 65 °C, MBA=0.05 wt.%

441 **4 Conclusion**

442 Through this study, we have successfully synthesized a biodegradable organic-inorganic SAP
443 with high content of non-toxic, low-cost, and natural abundantly available materials such as XG
444 polysaccharide and diatomite clay mineral, in the presence of AA as synthetic monomer. The SEM
445 micrographs showed that the surface morphology of XG-*g*-PAA/Diatomite SAP composite could be
446 beneficial for water penetration due to its loose and porous fracture surface compared to XG-*g*-PAA
447 composite. Under the optimized conditions *viz.* AA=15 g, neutralization degree=80%, APS=0.7
448 wt.%, XG=14 wt.%, diatomite=12 wt.%, reaction temperature 65°C, and MBA=0.05 wt.%, the
449 water absorption capacity of XG-*g*-PAA/Diatomite SAP composite in deionized water and 0.9 NaCl
450 saline solution was 1057.06 ± 69.53 g/g and 65.67 ± 5.43 g/g, respectively. Additionally, the results
451 revealed that the composite has excellent water retention capacity at various temperatures *i.e.* 45°C
452 and 60°C. Therefore, the above outcomes suggested that the XG-*g*-PAA/Diatomite SAP composite
453 which holds excellent swelling properties, is believed to find a wide ranges demanding applications
454 such as in hygienic products, agriculture and in waste water treatment. In this scenario, the authors

455 would like to recommend the extensive determination of biodegradability and biocompatibility of
456 this SAP composite to extend its proposed application fields. Thus, the findings of this approach
457 will hopefully provide a promising contribution to the alleviation of the environmental issues in
458 concern, through the use of low-cost and environmental friendly materials in SAP preparation
459 industries.

460 **Acknowledgements**

461 We are very grateful for the financial supported provided by the Scientific Research
462 Foundation for the Returned Overseas Chinese Scholars (State Education Ministry,
463 2010-1174), China Spark Program (Ministry of Science and Technology, 2013GA740073) and self-
464 determined research of CCNU from the fundamental research funds for the central universities
465 (CCNU15A02087). The authors would also like to extend their appreciations to Mr. Biebing Lin
466 from Wuhan University, College of Chemistry, for XRD test assistance.

467

468

469

470

471

472

473

474

Reference

1 M. S. Islam, M. S. Rahaman and J. H.Yeum, *Carbohydr. Polym.,* 2015, **115**, 69-77.

2 J. H. Trivedi, J. R.Jivani, K. H. Patel and H. C.Trivedi, *Chin. J. Polym. Sci.,* 2013, **31**, 1670-1684.

3 Y. Seki, A. Altinisik, B. Demircioğlu and C. Tetik, *Cellulose,* 2014, **21**, 1689-1698.

4 M. J. Zohuriaan-Mehr and K. Kabiri, *Iran. Polym. J.*, 2008, **17**, 451.

5 Zhang, Q.Wang and A.Wang, *Carbohydr. Polym.,* 2007, **68**, 367-374.

6 E. Feng, G. Ma, Y. Wu, H.Wang and Z. Lei, *Carbohydr. Polym.,* 2014, **111**, 463-468.

7 H. Dong, Q. Xu, Y. Li, S. Mo, S. Cai and L. Liu, *Colloids Surf., B: Biointerfaces,* 2008, **66**, 26-33.

8 A. Pourjavadi and G. R.Mahdavinia, *Turk. J. Chem.,* 2006, **30**, 595.

9 K. Haraguchi,; H.J. Li, K. Matsuda, T. Takehisa and E. Elliott, *Macromolecules,* 2005, **38**, 3482-3490.

10 M. Yadav and K. Y. Rhee, *Carbohydr. Polym.,* 2012, **90**, 165-173.

11 E. M. Ahmed, *Journal of Advanced Research* **2013**.

12 Y. Li, G. Huang, X. Zhang, B. Li, Y. Chen, T. Lu, T. J. Lu, and F. Xu, *Adv. Funct. Mater.,* 2013, **23**, 660-672.

13. H. Arslan, Block and Graft Copolymerization by Controlled/Living Radical Polymerization Methods, *Edited by Ailton De Souza Gomes,* 2012, 279.

14 A. Pourjavadi, R. Soleyman, H.Ghasemzadeh and H.Salimi, *Iranian. Polym., J.* 2010, **19**, 571-579.

15 X. Qi, M. Liu, Z. Chen and R. Liang, *Polym. Adv. Technol.,* 2007, **18**, 184-193.

16 B. Gao, P. Jiang, F. An, S. Zhao and Z. Ge, *Appl. Surf. Sci.,* 2005, **250**, 273-279.

17 J. F.Mukerabigwi, Q.Wang, X.Ma, M. Liu, S. Lei, H. Wei, X. Huang and Y. Cao, *J. Coat. Technol. Res.,* 2015, 1-10.

18 D. R. Nisbet, K. E. Crompton, S. D. Hamilton, S. Shirakawa, R. J. Prankerd and D. I. Finkelstein, *Biophys. Chem.* 2006, **121**, 14-20.

19 C. K. Simi and T. E. *Colloids Surf., B: Biointerfaces,* 2010, **81**, 513-520.

20 K. Nishinari, K.Yamatoya, and M. Shirakawa, *Handbook of hydrocolloids*: Woodhead Publishing, Cambridge, 2000. pp. 247–267.

21 H. S. Mahajan, V. Tyagi, G. Lohiya and P. Nerkar, *Drug Delivery,* 2012, **19**, 270-276.

22 H. S. Mahajan, and S. R.Deshmukh, *Carbohydr. Polym.,* 2015, **122**, 243-247.

23 J. Seo, T. Akaike, Y. J. Choi, M. Shirakawa, I. K. Kang and C. S.Cho, *Biomaterials* 2005, **26**, 3607-3615.

24 A. Mishra, *J. Biobased Mater. Bio.,* 2013, **7**, 12-18.

25 K. Sharma, B. Kaith, V. Kumar, S. Kalia, V. Kumar, and H. Swart, *Geoderma,* 2014, **232**, 45-55.

26 A. Pourjavadi, A. M. Harzandi and H. Hosseinzadeh, *Eur. Polym. J.,* 2004, **40**, 1363-1370.

27 M. M. Kenisarin and K. M. Kenisarina, *Renew. Sust. Energ. Rev.,* 2012, **16**, 1999-2040.

28 Z. Sun,; X.Yang, G. Zhang, S. Zheng and R. L. Frost, *Int. J. Miner. Process.,* 2013, **125**, 18-26.

29 W. Wang, and A.Wang, *Carbohydr. Polym.,* 2009, **77**, 891-897.

30 B. Song, W. Chen, Z. Liu, and S. Erhan, *Int. J. Plasticity,* 2006, **22**, 1549–1568.

31 R. Liang, H. Yuan, G. Xi and Q. Zhou, *Carbohydr. Polym.,* 2009, **77**, 181-187.

32 S. Hua, and A.Wang, *Carbohydr. Polym.,* 2009, **75**, 79-84.

33 H. Ismail,; M. Irani and Z. Ahmad, *J. Appl. Polym. Sci.,* 2012, **127**, 4195-4202.

34 A. Li and A. Wang, *Eur. Polym. J.,* 2005, **41**, 1630-1637.

35 A. Li, A. Wang, J. Chen, *J. Appl. Polym. Sci.,* 2004, **92**, 1596-1603.

36 Q. Tang, J. Lin, J. Wu and Y. Xu, *J. Appl. Polym. Sci.,* 2007, **104**, 735-739.

37 F. L. Buchholz, and N. A. Peppas, *J. Am. Chem. Soc.,* 1994.

38 P. J. Flory, *Principles of polymer chemistry*, Cornell University Press, 1953.

39 P. Lanthong, R. Nuisin,; S. Kiatkamjornwong, *Carbohydr. Polym.,* 2006, **66**, 229-245.

40 C. Spagnol, F. A. Rodrigues, A. B. Pereira, A. Fajardo, A. Rubira and E. Muniz, *Cellulose,* 2012, **19**, 1225-1237.

41 A. Li, J.Zhang and A.Wang, *Bioresour. Technol.,* 2007, **98**, 327-332.

42 E. Feng, G. Ma and Y. Wu, *Carbohydr. Polym.,* 2014, **111**, 463-468.

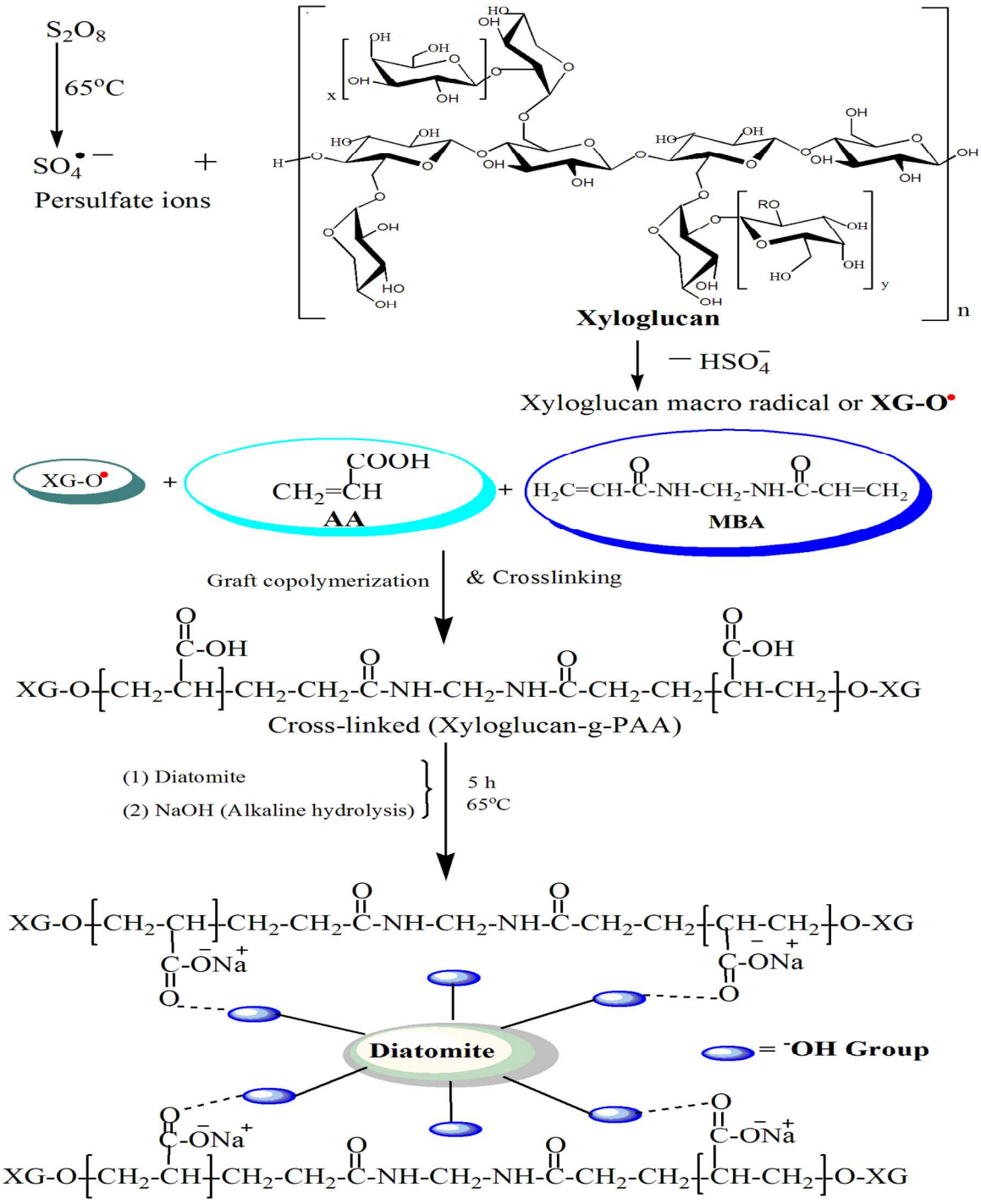

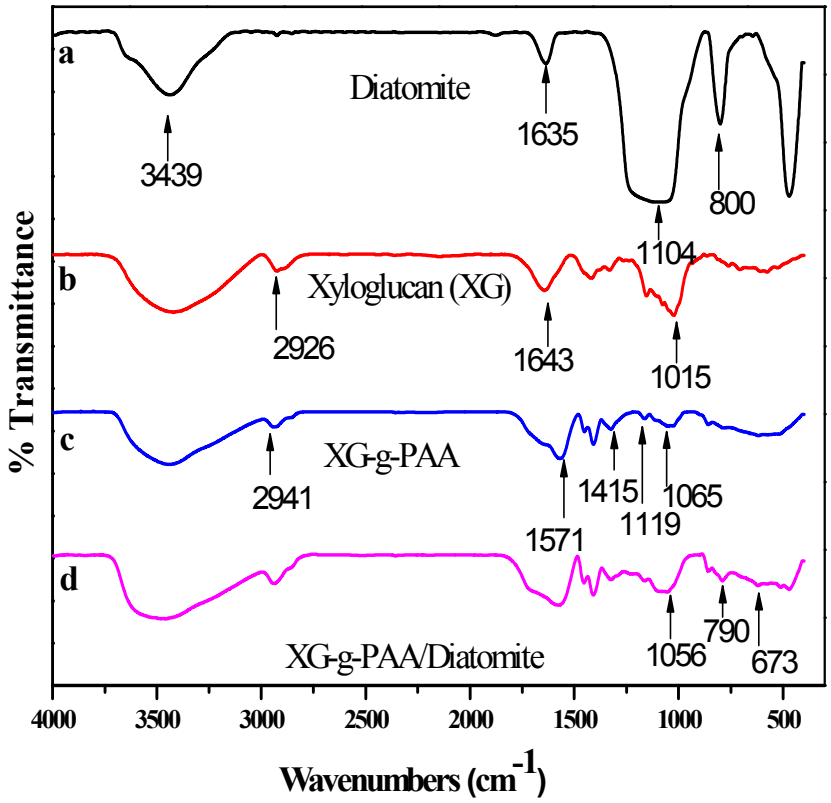

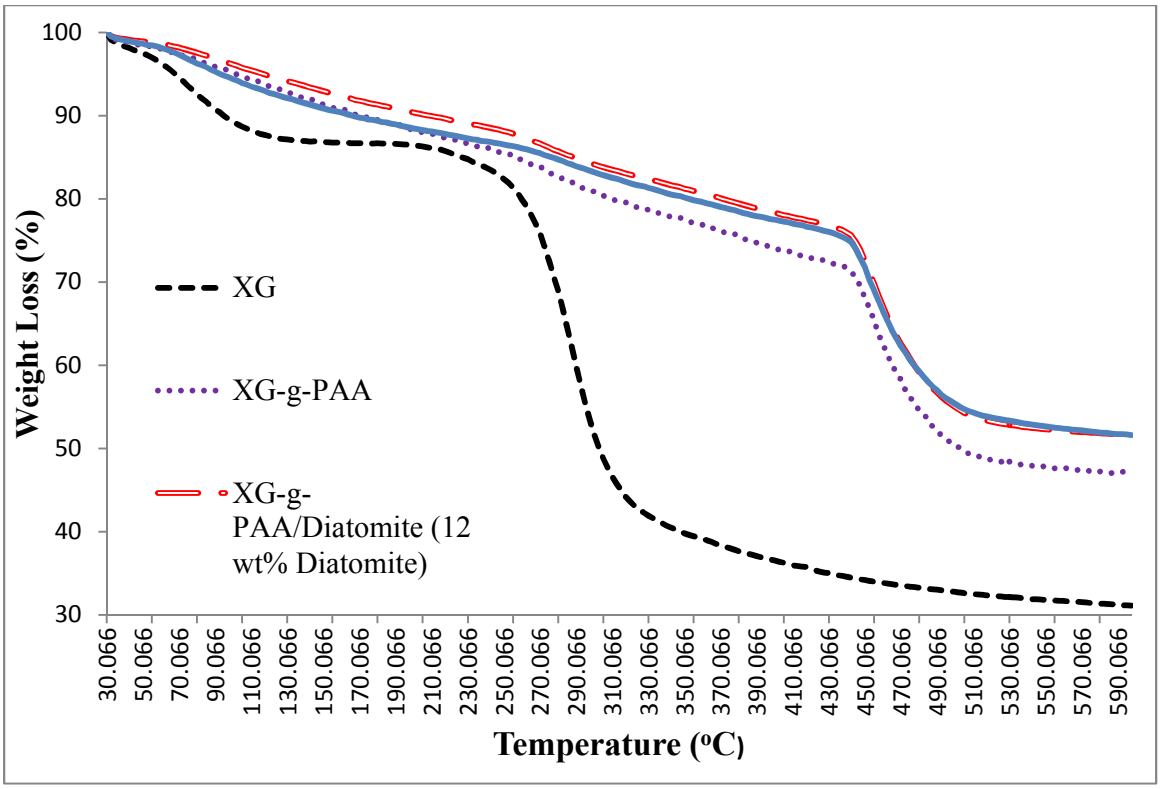

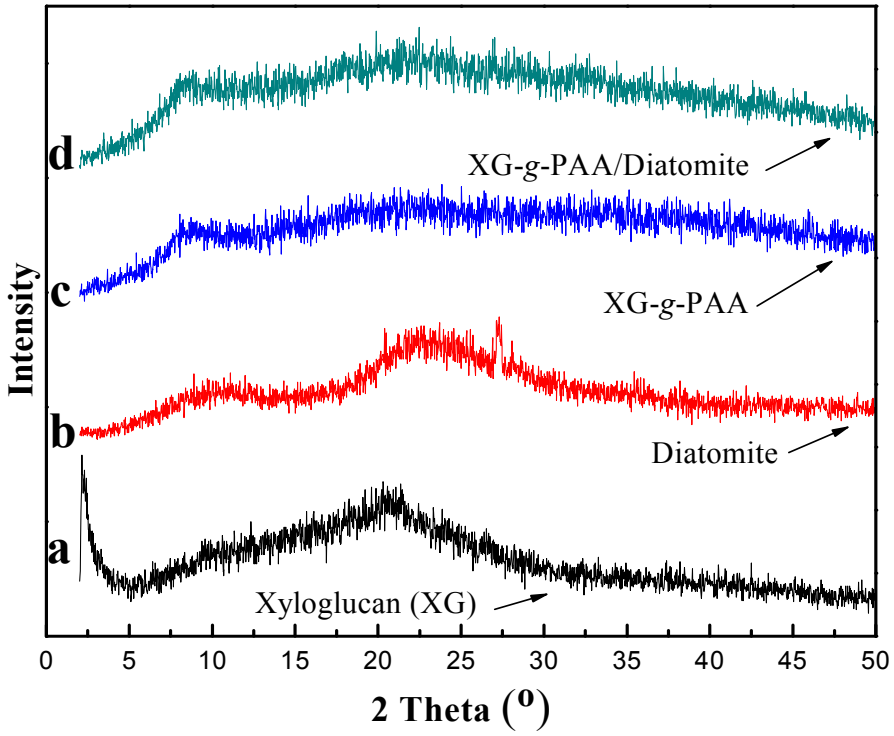

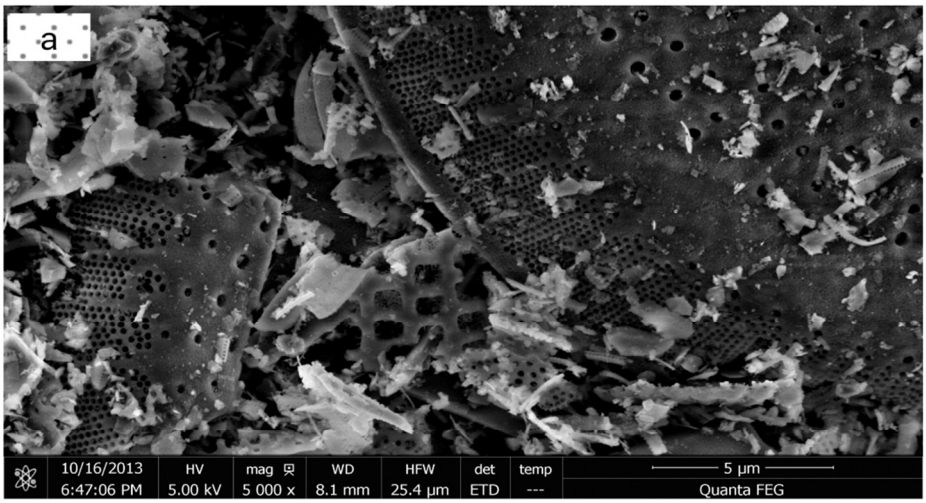

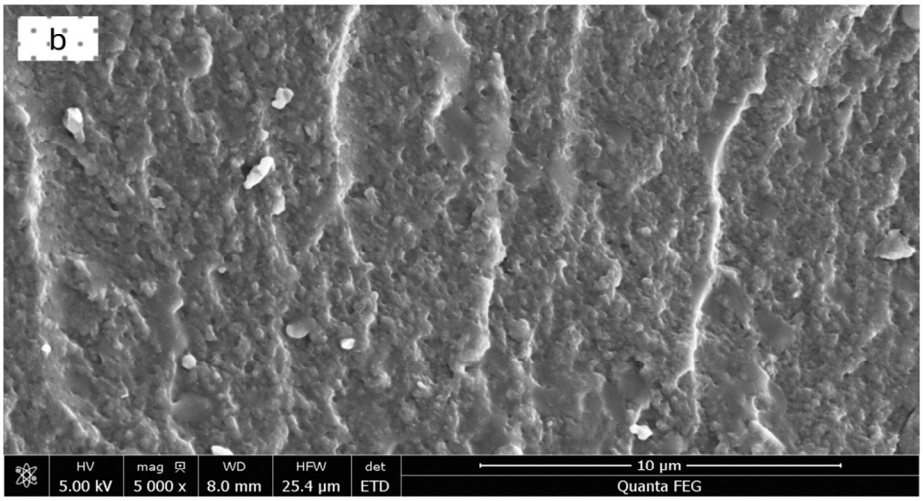

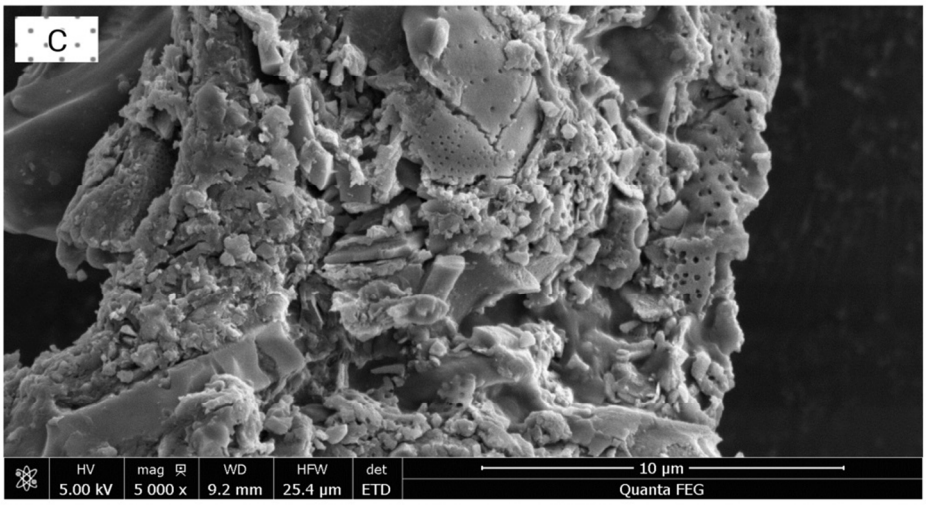

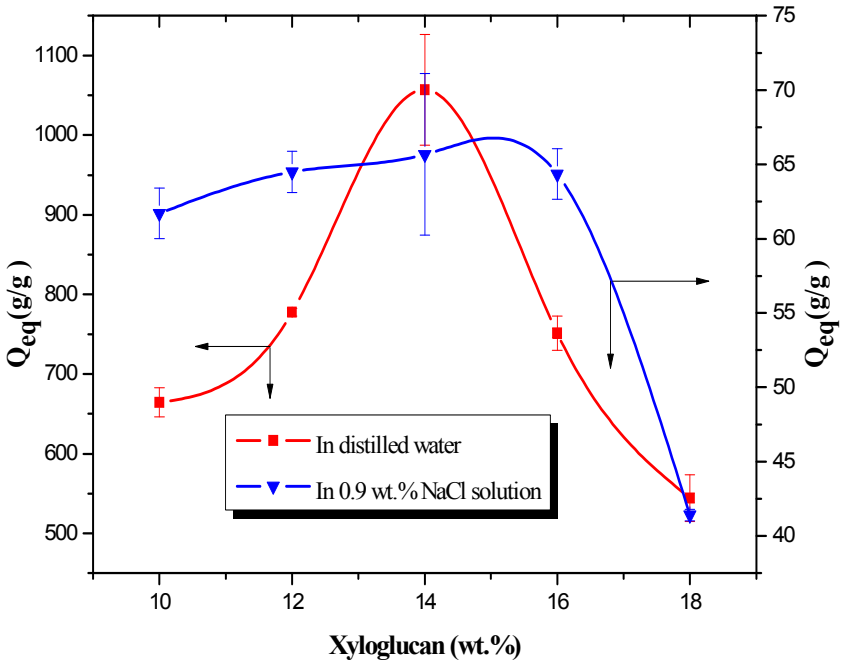

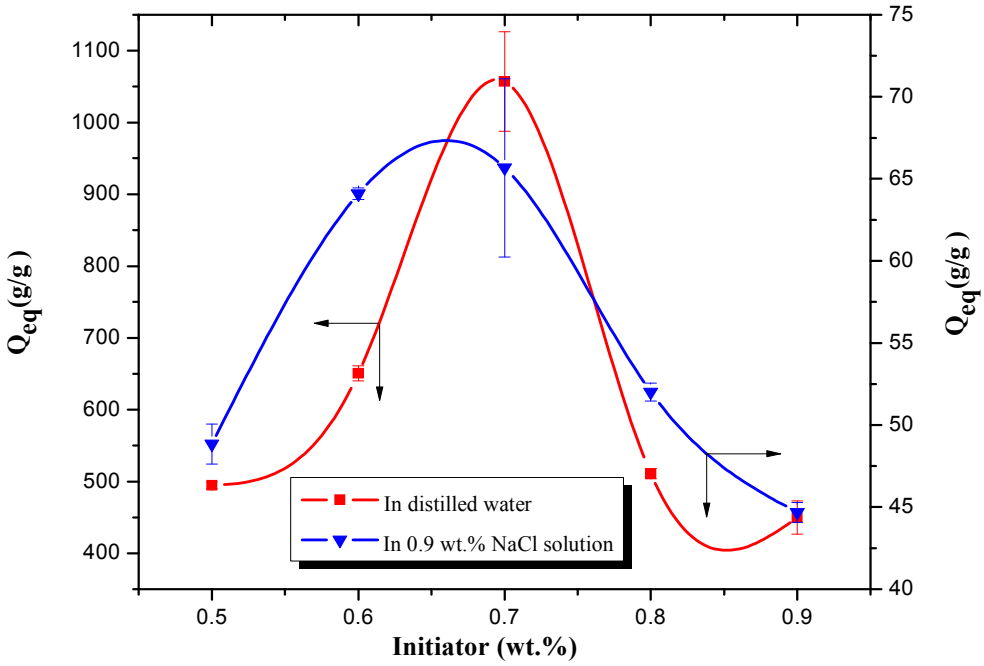

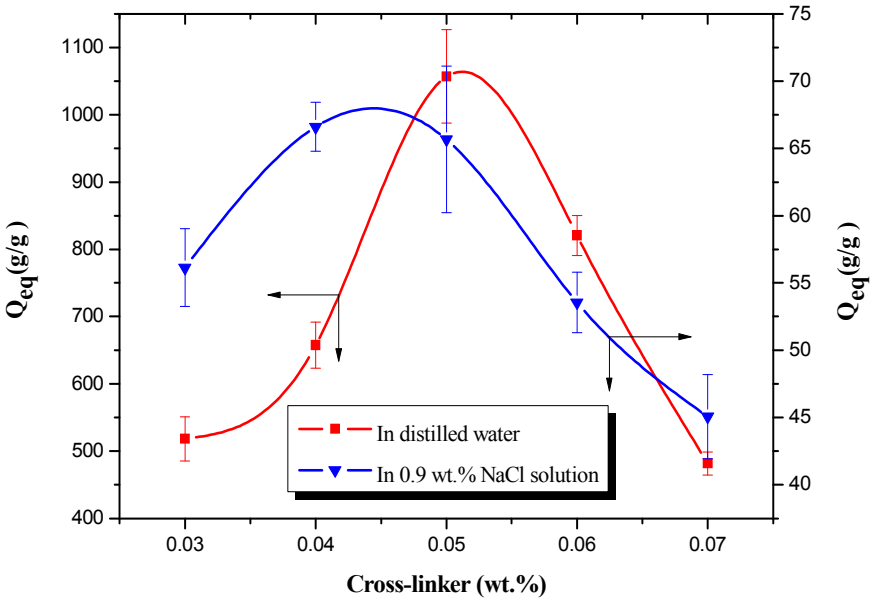

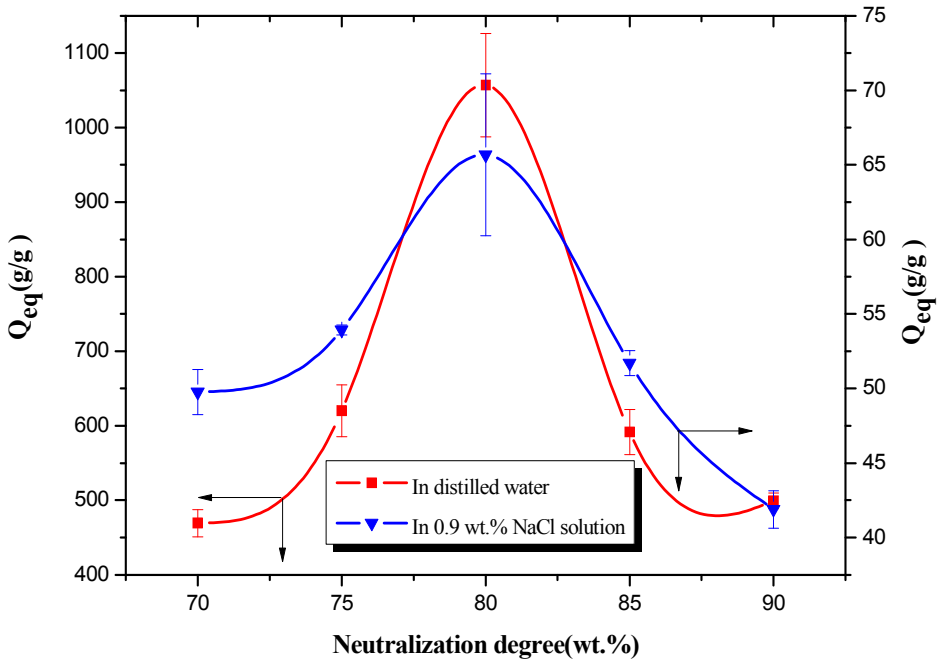

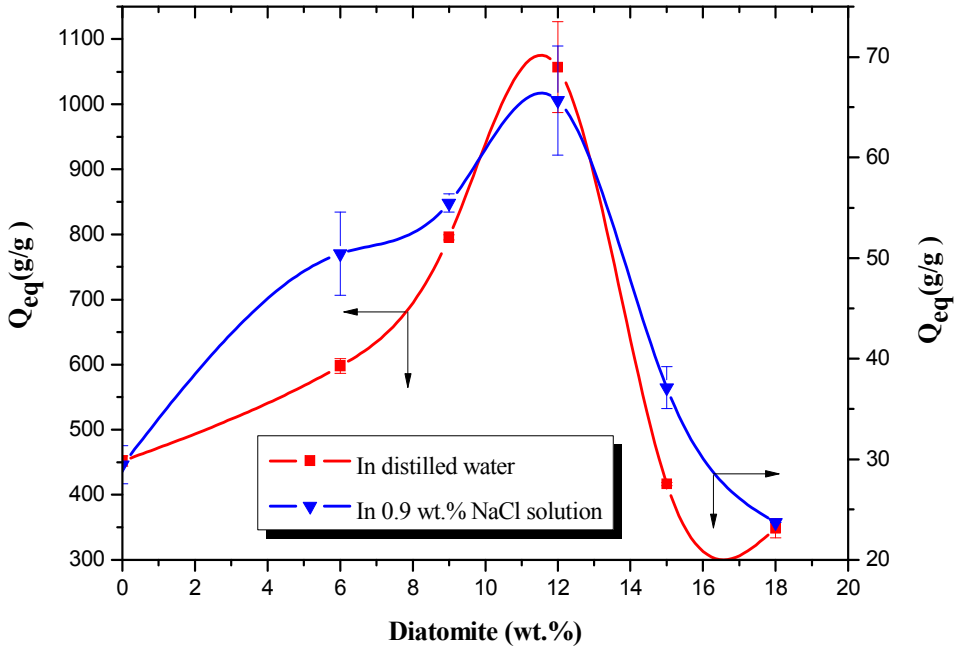

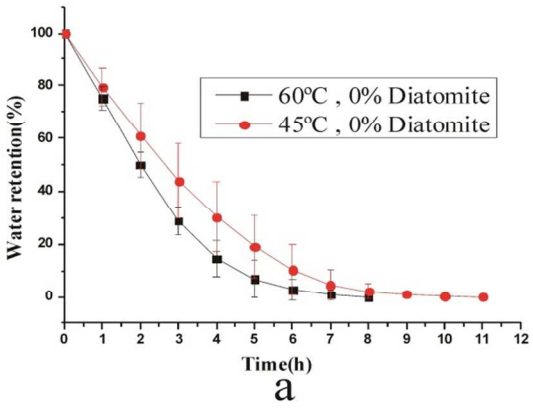

a

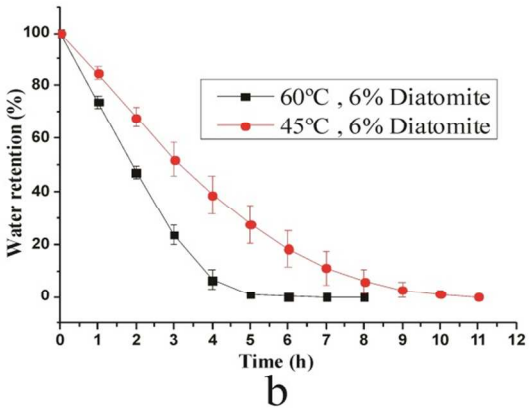

b

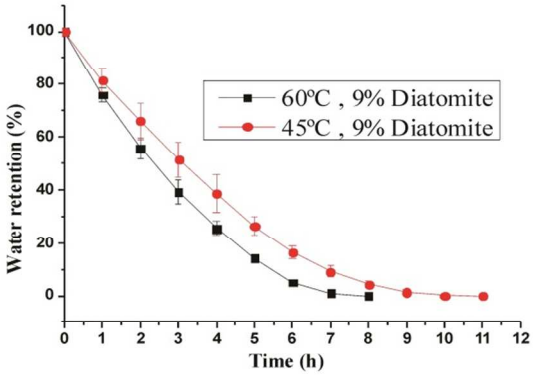

c

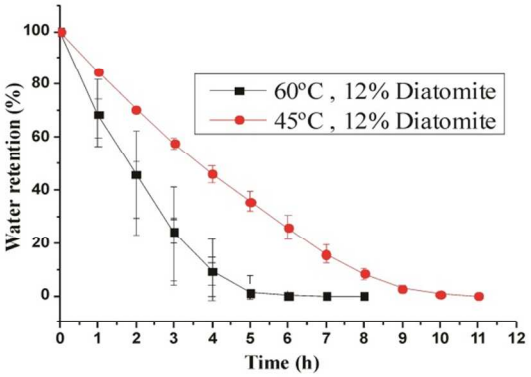

d

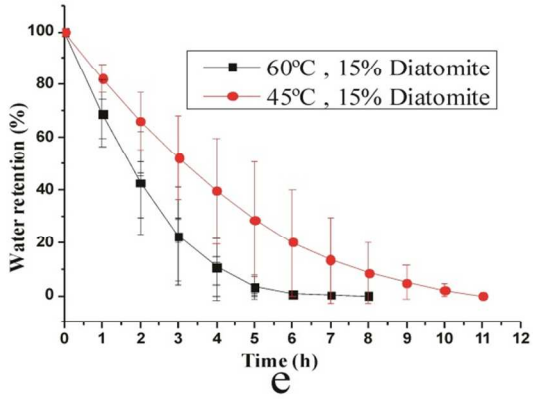

e

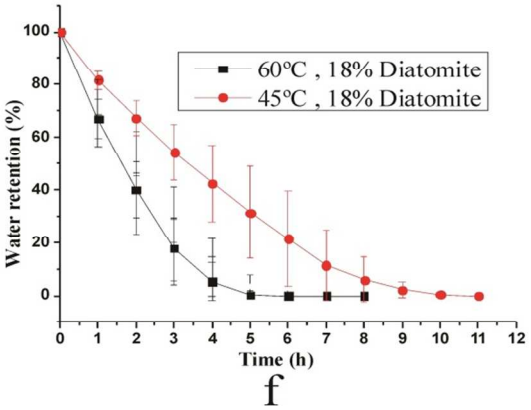

f

Figure captions

Scheme I. Proposed mechanism pathway for the synthesis of biodegradable organic-inorganic SAP (XG-*g*-PAA/Diatomite) superabsorbent composite through graft copolymerization

Fig.1: The FTIR spectra of (a) Diatomite, (b)XG, (c) XG-*g*-PAA, (d) XG-*g*-PAA/Diatomite (12 wt.%).

Fig. 2: TGA curves of XG, XG-*g*-PAA, XG-g-PAA/Diatomite (12 wt.% diatomite), and XG-*g*-PAA/Diatomite (18 wt.% diatomite)

Fig. 3: XRD diffraction patterns of (a) XG, (b) Diatomite, (c) XG-*g*-PAA, and (d) XG-*g*-PAA/Diatomite (12 wt.% Diatomite)

Fig. 4: Scanning Electron Micrographs of (a) Diatomite, (b) XG-*g*-PAA, and (c) XG-*g*-PAA/Diatomite (12 wt.%)

Fig. 5: Effect of XG content on the water absorbency. (Data were given as means ± SD (n = 3)). AA=15 g, diatomite=12 wt.%, MBA=0.05 wt.%, APS=0.7 wt.%, reaction temperature 65°C, neutralization degree=80%

Fig. 6: Effect of initiator (APS) content on the water absorbency. (Data were given as means ± SD (n = 3)). AA=15 g, diatomite=12 wt.%, MBA=0.05 wt.%, XG=14 wt.%, reaction temperature 65°C, neutralization degree=80%

Fig. 7: Effect of Cross-linker (MBA) content on the water absorbency. (Data were given as means ± SD (n=3)). AA=15 g, diatomite=12 wt.%, APS=0.7 wt.%, XG=14 wt.%, reaction temperature=65°C, neutralization degree=80%

Fig. 8: Effect of AA neutralization percentage on the water absorbency. (Data were given as means ± SD (n = 3)). AA=15 g, diatomite=12 wt.%, APS=0.7 wt.%, XG=14 wt.%, reaction temperature 65°C, MBA=0.05 wt.%

Fig. 9: Effect of clay content (diatomite) on the water absorbency. (Data were given as means ± SD (n = 3)). AA=15 g, neutralization degree=80%, APS=0.7 wt.%, XG=14 wt.%, reaction temperature 65°C, MBA=0.05 wt.%

Fig. 10: Water-retention properties of XG-*g*-PAA/Diatomite SAP prepared with various amount of diatomite at 45°C and 60°C. (a): 0 wt.% diatomite; (b): 6 wt.% diatomite; (c): 9 wt.% diatomite; (d): 12 wt.% diatomite; (e): 15 wt.% diatomite; (f): 18 wt.% diatomite. (Data were given as means ± SD (n = 3)). AA=15 g, neutralization degree=80%, APS=0.7 wt.%, XG=14 wt.%, reaction temperature 65 °C, MBA=0.05 wt.%